Model of the Second Most Abundant Cisplatin−DNA Cross-Link: X-ray Crystal Structure and Conformational Analysis of *cis*-[$(NH_3)_2$Pt(9-MeA-*N7*)(9-EtGH-*N7*)]$(NO_3)\cdot 2H_2O$ (9-MeA = 9-Methyladenine; 9-EtGH = 9-Ethylguanine)

Guy Schröder,[1a] Jirí Kozelka,*[,1b] Michal Sabat,*[,1c] Marie-Hélène Fouchet,[1b] Rut Beyerle-Pfnür,[1a] and Bernhard Lippert*[,1a]

Fachbereich Chemie, Universität Dortmund, 44221 Dortmund, Germany, Laboratoire de Chimie et Biochimie Pharmacologiques et Toxicologiques, Université René Descartes, 75270 Paris Cedex 06, France, and Department of Chemistry, University of Virginia, Charlottesville, Virginia 22901

Received June 15, 1995[⊗]

A model compound of the second most abundant DNA adduct of the antitumor agent cisplatin has been synthesized and structurally and spectroscopically characterized and its conformational behavior examined: *cis*-[$(NH_3)_2$Pt(9-MeA-*N7*)(9-EtGH-*N7*)]$(NO_3)_2\cdot 2H_2O$ (9-MeA = 9-methyladenine; 9-EtGH = 9-ethylguanine) crystallizes in the monoclinic system, space group $P2_1/n$ (No. 14) with $a = 7.931(2)$, $b = 11.035(3)$, $c = 26.757(6)$ Å, $\beta = 94.94(2)°$, and $Z = 4$. The two purine bases adopt a *head-to-head* orientation, with NH_2 of 9-MeA and CO of 9-EtGH being at the same side of the Pt coordination plane. A theoretical conformational analysis of the complex *cis*-[$(NH_3)_2$Pt(Ade)(Gua)]$^{2+}$ (Ade = adenine; Gua = guanine) based on molecular mechanics calculations of the nonbonded energy has revealed four minimum-energy zones similar to those derived previously for *cis*-[$(NH_3)_2$Pt$(Gua)_2$]$^{2+}$ (Kozelka; et al. *Eur. J. Biochem.* **1992**, *205*, 895). This conformational analysis has allowed, together with the calculation of chemical shifts due to ring effects, the attribution of the two conformers observed for *cis*-[$(NH_3)_2$Pt{d(ApG)}]$^+$ by Dijt et al. (*Eur. J. Biochem.* **1989**, *179*, 344) to the two *head-to-head* conformational zones. The orientation of the two nucleobases in the crystal structure of *cis*-[$(NH_3)_2$Pt(9-MeA)(9-EtGH)]$^{2+}$ corresponds, according to our analysis, roughly to that preferentially assumed by the minor rotamer of *cis*-[$(NH_3)_2$Pt{d(ApG)}]$^+$.

Introduction

The d(ApG) intrastrand N7,N7 cross-link represents the second most abundant DNA adduct of the antitumor agent *cis*-$(NH_3)_2PtCl_2$ (cisplatin, *cis*-DDP), accounting for *ca.* 20−30% of all lesions.[2,3] The major adduct is the d(GpG) intrastrand crosslink, which makes up to 60%. Biological effects of these two main adducts are apparently different. For example, the d(GpG) adduct inhibits several DNA polymerases[4] and RNA polymerases[5] more severly than the d(ApG) adduct, yet the less abundant d(ApG) cross-link has been found to be more mutagenic by a factor of 5−10 as compared to the d(GpG) cross-link.[6,7] Distortion of the DNA double helix has been reported to be different as well.[8]

Considering the rather similar geometries of adenine and guanine nucleobases (from a viewpoint of N7 metal coordination), there is no straightforward reason as to why bis(guanine) and mixed adenine, guanine adducts should lead to structurally different DNA distortions and different biological consequences. On the other hand, it has previously been shown that one of the principal structural parameters by which platinum bis(purine) complexes can differ are the torsional angles about the Pt−N7 bonds, α and β (Figure 1).[9] These torsional angles can be indirectly deduced from the chemical shifts of the aromatic protons.[9]

While the d(GpG) cross-link has been studied intensively[10] both in model systems, such as *cis*-[$(NH_3)_2$Pt(9-EtGH)$_2$]$^{2+}$,[11] *cis*-[$(NH_3)_2$Pt$(Guo)_2$]$^{2+}$,[12] *cis*-[$(NH_3)_2$Pt(5'-GMP)$_2$]$^{2+}$,[13] *cis*-[$(NH_3)_2$Pt{d(GpG}]$^+$,[14] and *cis*-$(NH_3)_2$Pt{d(pGpG)},[15] and single-[16] and double-stranded[17] oligonucleotide adducts, very few studies have focused on structural properties of ApG adducts of *cis*-DDP.[18] In particular, no structural data on this cross-

⊗ Abstract published in *Advance ACS Abstracts,* February 1, 1996.

(1) (a) University of Dortmund. (b) Université René Descartes. (c) University of Virginia.
(2) Fichtinger-Schepman, A. M. J.; van der Veer, J. L.; den Hartog, J. H. J.; Lohman, P. H. M.; Reedijk, J. *Biochemistry* **1985**, *24*, 707.
(3) (a) Eastman, A. *Biochemistry* **1983**, *22*, 3927. (b) Eastman, A. *Biochemistry* **1985**, *24*, 5027. (c) Eastman, A. *Pharmacol. Ther.* **1987**, *34*, 155.
(4) Comess, K. M.; Burstyn, J. N.; Essigmann, J. M.; Lippard, S. J. *Biochemistry* **1992**, *31*, 3975.
(5) Corda, Y.; Anin, M.-F.; Leng, M.; Job, D. *Biochemistry* **1992**, *31*, 1904.
(6) (a) Burnouf, D.; Daune, M.; Fuchs, R. P. P. *Proc. Natl. Acad. Sci. U.S.A.* **1987**, *84*, 3758. (b) Burnouf, D.; Gauthier, C.; Chottard, J. C.; Fuchs, R. P. P. *Proc. Natl. Acad. Sci. U.S.A.* **1990**, *87*, 6087.
(7) For a discussion of this subject, see also: Lippert, B.; Schöllhorn, H.; Thewalt, U. *Inorg. Chim. Acta* **1992**, *198*−200, 723.
(8) (a) Marrot, L.; Leng, M. *Biochemistry* **1989**, *28*, 1454. (b) Schwartz, A.; Marrot, L.; Leng, M. *Biochemistry* **1989**, *28*, 7975.
(9) Kozelka, J.; Fouchet, M. H.; Chottard, J. C. *Eur. J. Biochem.* **1992**, *205*, 895.
(10) For a recent summary on structural aspects, see: Yao, S.; Plastaras, J. P.; Marzilli, L. G. *Inorg. Chem.* **1994**, *33*, 6061.
(11) (a) Lippert, B.; Raudaschl, G.; Lock, C. J. L.; Pilon, P. *Inorg. Chim. Acta* **1984**, *93*, 43. (b) Schöllhorn, H.; Raudaschl-Sieber, G.; Müller, G.; Thewalt, U.; Lippert, B. *J. Am. Chem. Soc.* **1985**, *107*, 5932.
(12) Cramer, R.; Dahlstrom, P. L.; Seu, M. J. T.; Norton, T.; Kashiwagi, M. *Inorg. Chem.* **1980**, *19*, 148.
(13) (a) Marzilli, L. G.; Chalilpoyil, P.; Chiang, C. C.; Kistenmacher, T. J. *J. Am. Chem. Soc.* **1980**, *102*, 2480. (b) Kistenmacher, T. J.; Chiang, D. D.; Chalilpoyil, P.; Marzilli, L. G. *J. Am. Chem. Soc.* **1979**, *101*, 1143.
(14) (a) Girault, J. P.; Chottard, G.; Lallemand, J. Y.; Chottard, J. C. *Biochemistry* **1982**, *21*, 1352. (b) den Hartog, J. H. J.; Altona, C.; Chottard, J. C.; Girault, J. P.; Lallemand, J. Y.; de Leeuw, F. A. A. M.; Marcelis, A. T. M.; Reedijk, J. *Nucleic Acids Res.* **1982**, *10*, 4715.
(15) (a) Sherman, S. E.; Gibson, D.; Wang, A. H.-J.; Lippard, S. J. *Science* **1985**, *230*, 412. (b) Sherman, S. E.; Gibson, D.; Wang, A. H.-J.; Lippard, S. J. *J. Am. Chem. Soc.* **1988**, *110*, 7368. (c) Coll, M.; Sherman, S. E.; Gibson, D.; Lippard, S. J.; Wang, A. H.-J. *J. Biomol. Struct. Dyn.* **1990**, *8*, 315.

0020-1669/96/1335-1647$12.00/0

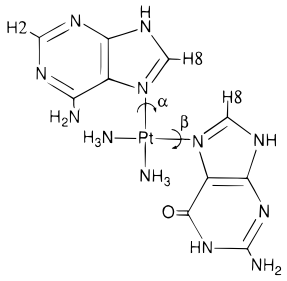

Figure 1. The complex *cis*-$[(NH_3)_2Pt(Ade)(Gua)]^{2+}$ in a reference conformation where the two bases are coplanar with the platinum coordination plane. For this conformation, the torsion angles α and β are defined as zero. Positive values of α and β correspond to counterclockwise rotations with respect to this reference conformation.

link or a model thereof is presently available. Here we report the X-ray crystal structure of a model compound containing 9-methyladenine (9-MeA) and 9-ethylguanine (9-EtGH), together with spectroscopic and conformational studies.

Experimental Section

Preparation. *cis*-$[(NH_3)_2Pt(9\text{-EtGH})Cl]Cl$[19] was treated with 2 equiv of $AgNO_3$ in water (typically 0.8−1 mmol in 30−40 mL) in the dark at room temperature for 2 h. After addition of 1 equiv of 9-MeA[20] the reaction mixture was stirred in the dark at room temperature for 2 days. The mixture was filtered to remove precipitated AgCl. The filtrate was concentrated to 2 mL, some $NaNO_3$ was added, and the solution was kept at 4 °C. The title compound was obtained as colorless crystals in 44% yield. Anal. Calcd for $[(NH_3)_2Pt(9\text{-MeA-}N7)(9\text{-EtGH-}N7)](NO_3)_2\cdot 2H_2O$, $C_{13}H_{26}N_{14}O_9Pt$: C, 21.76; H, 3.65; N, 27.33. Found: C, 21.7; H, 3.9; N, 27.8.

IR (cm^{-1}, selected bands only): 3354 b, 3091 b, 1690 vs, 1622 vs, 1386 vs, 1266 w, 1241 m, 1218 s, 839 s, 825 vs, 793 s, 774 s, 732 s, 732 s, 718 s. ^{195}Pt NMR (δ, D_2O), −2460 ppm.

According to ^1H NMR spectra (D_2O, pD 6), the reaction mixture also contains 10−15% of the linkage isomer *cis*-$[(NH_3)_2Pt(9\text{-MeA-}N1)(9\text{-EtGH-}N7)]^{2+}$. Isolation of this compound has not been achieved yet.

Instruments. The IR spectrum (KBr) was recorded on an IFS 113v Bruker spectrometer. ^1H NMR spectra were recorded on a Jeol JNM-FX 60 and a Bruker AC 200 spectrometer. Given shifts are relative to TMS in DMF-d_7 and relative to TSP in D_2O. The ^{195}Pt NMR spectrum (42.8 MHz) was recorded with K_2PtCl_6 as external standard. pK_a values were determined by plotting ^1H NMR chemical shifts vs the uncorrected pH (pH*).

Table 1. Crystallographic Data for *cis*-$[(NH_3)_2Pt(9\text{-MeA})(9\text{-EtGH})](NO_3)_2\cdot 2H_2O$

chem formula	$C_{13}H_{26}N_{14}O_9Pt$	temp, °C	−120
fw	717.5	λ, Å (Mo Kα)	0.710 69
space group	monoclinic, $P2_1/n$ (No. 14)	ρ(calc), g cm^{-3}	2.043
a, Å	7.931(2)	μ(Mo Kα), cm^{-1}	61.49
b, Å	11.035(3)	transm coeff	0.77−1.00
c, Å	26.757(6)	R^a	0.027
β, deg	94.94(2)	R^b	0.034
V, Å^3	2333(1)		
Z	4		

[a] $R = \sum(|F_o| - |F_c|)/\sum|F_o|$. [b] $R_w = [\sum w(|F_o| - |F_c|)^2/\sum w|F_o|^2]^{1/2}$. $w = 1/\sigma^2(F)$.

X-ray Analysis. Experimental details of the X-ray data collection, the structure solution and refinement as well as crystal data for the title compound are compiled in Table 1. The structure was solved by heavy atom methods (Patterson and Fourier maps) in TEXSAN 5.0.[21] Absorption corrections were applied by using the DIFABS program.[22] Final atomic coordinates and equivalent isotropic temperature factors, and anisotropic thermal parameters are included in the Supporting Information.

Molecular Mechanics Calculations. The nonbonded energy was calculated using the AMBER force-field[23] (eq 1). The Lennard−Jones

$$E = \sum_{\text{nonbonded}}\left(\frac{A}{r^{12}} - \frac{B}{r^{6}} + \frac{q_i q_j}{\epsilon_{ij} r_{ij}}\right) + \sum_{\text{H bonds}}\left(\frac{C}{r^{12}} - \frac{D}{r^{10}}\right) \qquad (1)$$

parameters A−D for the platinum-bound nucleobases were assumed to be the same as those of the bases within DNA, and the NH_3 ligands were equivalenced to the NH_3^+ groups of lysine. The atomic charges used were derived from *ab initio* calculations on *cis*-$[(NH_3)_2Pt(Gua)_2]^{2+}$ [24] and $[(NH_3)_3Pt(Ade)]^{2+}$,[25] and are listed in Table A1 in the Supporting Information. Since we have considered only rotamers with respect to the Pt−N7 bonds, the parameters utilized for the Pt atom are irrelevant. A distance-dependent dielectric coefficient $\epsilon = 4r_{ij}$ was used; no cutoff was applied.

Results and Discussion

Description of Structure. The title compound crystallizes in the centrosymmetric space group $P2_1/n$. Therefore, by definition, the crystral contains both enantiomers of the chiral cation of *cis*-$[(NH_3)_2Pt(9\text{-MeA-}N7)(9\text{-EtGH-}N7)](NO_3)_2\cdot 2H_2O$ in the unit cell. A view of one of the two enantiomeric cations is given in Figure 2. Selected interatomic distances and angles are listed in Table 2. Pt is bound via the N7 positions of the two purine bases which are oriented in a *head-to-head* fashion. Pt−N distances and angles about the metal are normal and compare well with other Pt(II) complexes of 9-EtGH[11] and 9-MeA[26] with N7 binding. Dihedral angles, as defined by Kozelka et al.[9] are 9-MeA/PtN_4, ±66.07° (α in Figure 1) and 9-EtGH/PtN_4, ∓88.26° (β in Figure 1). According to the convention introduced by Kistenmacher et al.[27] angles 9-EtGH/PtN_4 are 91.74° and 9-MeA/9-EtGH 92.09° (Figure 3). Thus

(16) (a) den Hartog, J. H. J.; Altona, C.; van der Marel, G. A.; Reedijk, J. *Eur. J. Biochem.* **1985**, *147*, 371. (b) Admiraal, G.; van der Veer, J. L.; De Graaff, R. A. G.; den Hartog, J. H. J.; Reedijk, J. *J. Am. Chem. Soc.* **1987**, *109*, 592. (c) Girault, J. P.; Chottard, J. C.; Neumann, J. M.; Tran-Dinh, S.; Huynh-Dinh, T.; Igolen, J. *Nouv. J. Chim.* **1984**, *8*, 7. (d) Girault, J. P.; Chottard, J. C.; Guittet, E. R.; Lallemand, J. Y.; Huynh-Dinh, T.; Igolen, J. *Biochem. Biophys. Res. Commun.* **1982**, *109*, 1157. (e) Caradonna, J. P.; Lippard, S. J. *Inorg. Chem.* **1988**, *27*, 1454. (f) den Hartog, J. H. J.; Altona, C.; van Boom, J. H.; van der Marel, G. A.; Haasnoot, C. A. G.; Reedijk, J. *J. Am. Chem. Soc.* **1984**, *106*, 1528.

(17) (a) den Hartog, J. H. J.; Altona, C.; van Boom, J. H.; van der Marel, G. A.; Hassnoot, C. A. G.; Reedijk, J. *J. Biomol. Struct. Dyn.* **1985**, *2*, 1137. (b) Herman, F.; Kozelka, J.; Stoven, V.; Guittet, E.; Girault, J. P.; Huynh-Dinh, T.; Igolen, J.; Lallemand, J. Y.; Chottard, J. C. *Eur. J. Biochem.* **1990**, *194*, 119. (c) Marzilli, L. G. *J. Inorg. Biochem.* **1991**, *43*, 425.

(18) (a) van Hemelryck, B.; Girault, J.-P.; Chottard, G.; Valadon, P.; Laoui, A.; Chottard, J.-C. *Inorg. Chem.* **1987**, *26*, 787. (b) Rice, J. A.; Crothers, D. M.; Pinto, A. L.; Lippard, S. J. *Proc. Natl. Acad. Sci. U.S.A.* **1988**, *85*, 4158. (c) Hambley, T. W. *J. Chem. Soc., Chem. Commun.* **1988**, 221. (d) Laoui, A.; Kozelka, J.; Chottard, J. C. *Inorg. Chem.* **1988**, *27*, 2751. (e) Hambley, T. W. *Inorg. Chem.* **1991**, *30*, 937. (f) Alink, M.; Nakahara, H.; Hirano, T.; Inagaki, K.; Nakanishi, M.; Kidani, Y.; Reedijk, J. *Inorg. Chem.* **1991**, *30*, 1236.

(19) Raudaschl, G.; Lippert, B. *Inorg. Chim. Acta* **1983**, *80*, L49.

(20) Krüger, G. *Z. Physiol. Chem.* **1983**, *18*, 434.

(21) *TEXSAN: Single Crystal Structure Analysis Software*; Version 5.0; Molecular Structure Corporation: The Woodlands, TX, 1989.

(22) Walker, N.; Stuart, D. *Acta Crystallogr., Sect. A* **1983**, *39*, 158.

(23) Weiner, S. J.; Kollman, P. A.; Nguyen, D. T.; Case, D. A. *J. Comput. Chem.* **1986**, *7*, 230.

(24) Kozelka, J.; Savinelli, R.; Berthier, G. Unpublished results.

(25) Kozelka, J.; Savinelli, R.; Berthier, G.; Flament, J. P.; Lavery, R. *J. Comp. Chem.* **1992**, *13*, 45.

(26) See, e.g.: (a) Beyerle-Pfnür, R.; Brown, B.; Faggiani, R.; Lippert, B.; Lock, C. J. L. *Inorg. Chem.* **1985**, *24*, 4001. (b) Beyerle-Pfnür, R.; Jaworski, S.; Lippert, B.; Schöllhorn, H.; Thewalt, U. *Inorg. Chim. Acta* **1985**, *107*, 217. (c) Iakovidis, A.; Hadjiliadis, N.; Dahan, F.; Laussac, J.-P.; Lippert, B. *Inorg. Chim. Acta* **1990**, *175*, 57. (d) Krizanovic, O.; Sabat, M.; Beyerle-Pfnür, R.; Lippert, B. *J. Am. Chem. Soc.* **1993**, *115*, 5538.

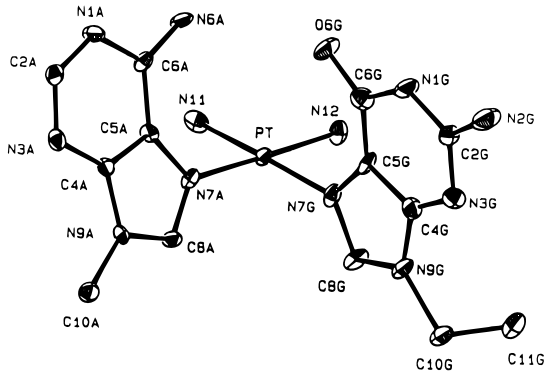

Figure 2. View of cation of *cis*-$[(NH_3)_2Pt(9\text{-MeA-}N7)(9\text{-EtGH-}N7)](NO_3)_2\cdot 2H_2O$ with atom numbering scheme.

Table 2. Selected Interatomic Distances (Å) and Angles (deg)

Pt−N(7G)	2.006(8)	N(3A)−C(2A)	1.31(1)
Pt−N(7A)	2.036(7)	N(3A)−C(4A)	1.34(1)
Pt−N(11)	2.033(8)	N(6A)−C(6A)	1.32(1)
Pt−N(12)	2.032(7)	N(7G)−C(5G)	1.38(1)
O(1)−N(1)	1.24(1)	N(7G)−C(8G)	1.35(1)
O(2)−N(1)	1.26(1)	N(7A)−C(5A)	1.38(1)
O(3)−N(1)	1.22(1)	N(7A)−C(8A)	1.34(1)
O(4)−N(2)	1.25(1)	N(9G)−C(4G)	1.38(1)
O(5)−N(2)	1.23(1)	N(9G)−C(8G)	1.33(1)
O(6G)−C(6G)	1.26(1)	N(9G)−C(10G)	1.53(1)
O(6)−N(2)	1.21(1)	N(9A)−C(4A)	1.38(1)
N(1G)−C(2G)	1.34(1)	N(9A)−C(8A)	1.34(1)
N(1G)−C(6G)	1.43(1)	N(9A)−C(10A)	1.45(1)
N(1A)−C(2A)	1.36(1)	C(4G)−C(5G)	1.39(1)
N(1A)−C(6A)	1.33(1)	C(4A)−C(5A)	1.38(1)
N(2G)−C(2G)	1.35(1)	C(5G)−C(6G)	1.37(1)
N(3G)−C(2G)	1.33(1)	C(5A)−C(6A)	1.43(1)
N(3G)−C(4G)	1.34(1)	C(10G)−C(11G)	1.50(1)

N(7G)−Pt−N(7A)	90.3(3)	C(4A)−N(9A)−C(10A)	126.6(7)
N(7G)−Pt−N(11)	176.0(3)	C(8A)−N(9A)−C(10A)	125.4(8)
N(7G)−Pt−N(12)	88.8(3)	N(1G)−C(2G)−N(2G)	117.4(8)
N(7A)−Pt−N(11)	92.1(3)	N(1G)−C(2G)−N(3G)	125.4(8)
N(7A)−Pt−N(12)	178.0(3)	N(2G)−C(2G)−N(3G)	117.0(9)
N(11)−Pt−N(12)	88.9(3)	N(1A)−C(2A)−N(3A)	128.4(9)
O(1)−N(1)−O(2)	117(1)	N(3G)−C(4G)−N(9G)	127(1)
O(1)−N(1)−O(3)	122(1)	N(3G)−C(4G)−C(5G)	128.2(9)
O(2)−N(1)−O(3)	121(1)	N(9G)−C(4G)−C(5G)	104.3(8)
C(2G)−N(1G)−C(6G)	124.0(8)	N(3A)−C(4A)−N(9A)	127.4(8)
C(2A)−N(1A)−C(6A)	119.7(8)	N(3A)−C(4A)−C(5A)	127.0(8)
O(4)−N(2)−O(5)	117(1)	N(9A)−C(4A)−C(5A)	105.5(7)
O(4)−N(2)−O(6)	121(1)	N(7G)−C(5G)−C(4G)	109.0(8)
O(5)−N(2)−O(6)	122(1)	N(7G)−C(5G)−C(6G)	131.0(8)
C(2G)−N(3G)−C(4G)	110.9(9)	C(4G)−C(5G)−C(6G)	120.0(8)
C(2A)−N(3A)−C(4A)	111.3(8)	N(7A)−C(5A)−C(4A)	109.4(7)
Pt−N(7G)−C(5G)	128.6(6)	N(7A)−C(5A)−C(6A)	134.4(8)
Pt−N(7G)−C(8G)	124.6(7)	C(4A)−C(5A)−C(6A)	116.2(8)
C(5G)−N(7G)−C(8G)	106.6(7)	O(6G)−C(6G)−N(1G)	117.7(9)
Pt−N(7A)−C(5A)	126.5(6)	O(6G)−C(6G)−C(5G)	131(1)
Pt−N(7A)−C(8A)	127.4(6)	N(1G)−C(6G) C(5G)	111(1)
C(5A)−N(7A)−C(8A)	106.1(7)	N(1A)−C(6A)−N(6A)	119.1(8)
C(4G)−N(9G)−C(8G)	110.3(8)	N(1A)−C(6A)−C(5A)	117.1(8)
C(4G)−N(9G)−C(10G)	124.7(8)	N(6A)−C(6A)−C(5A)	123.7(8)
C(8G)−N(9G)−C(10G)	125.0(8)	N(7G)−C(8G)−N(9G)	109.7(8)
C(4A)−N(9A)−C(8A)	108.0(7)	N(7A)−C(8A)−N(9A)	111.0(8)
N(9G)−C(10G)−C(11G)	110.1(8)		

guanine and adenine planes are practically at right angle, and guanine is at the same time almost perpendicular to the Pt coordination plane, while 9-MeA is substantially tilted with respect to the PtN_4 plane. Deviations of Pt from nucleobase and coordination planes are moderate to small, e.g. 0.097 Å from the best plane of 9-MeA, 0.022 Å from that of 9-EtGH, and 0.011 Å from the N_4 plane.

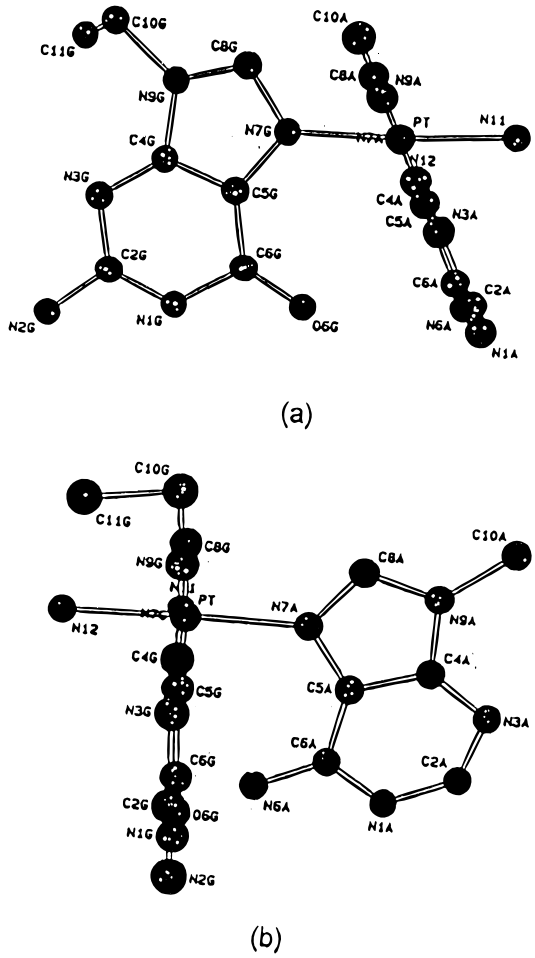

Figure 3. Conformational drawings of the cation showing (a) the angle between 9-MeA and the PtN_4 plane and (b) the dihedral angle between the two purine bases.

The intramolecular distance between O6 (guanine) and N6 (adenine) is 3.11 Å, suggesting a relatively weak H bonding interaction. H atoms, as located in Fourier maps, indicate a N6(A)−H6−O6(G) angle of 111.1° and distances of 0.95 Å for N6(A)−H6 and 2.64 Å for H6···O6(G).

^{1}H NMR Spectra. At ambient temperature, the ^{1}H NMR spectrum (D_2O, pD 6, $c_{Pt} \approx 0.04$ M) of the title compound consists of the following resonances: 9-MeA, H8, 8.72 ppm, s; H2, 8.25 ppm, s; CH_3 3.88 ppm, s; 9-EtGH, H8, 8.19 ppm, s; CH_2, 4.03 ppm, q; CH_3, 1.32 ppm, t. If a low-field NMR spectrometer (60 MHz) is used, both adenine H8 and guanine H8 resonances display ^{195}Pt satellites with ^3J values of 23.2 and 25.2 Hz, respectively.[28] A concentration dependence of the ^{1}H NMR resonances (D_2O, pD ≈ 4.4) in the range 0.003 M $< c_{Pt} <$ 0.07 M shows an influence on H2 of 9-MeA only (Supporting Information). In the given range, H2 moves upfield with increasing concentration, by ca 0.09 ppm. This shift is a consequence of intermolecular stacking occurring between platinated purines, most likely the 9-MeA rings of two cations. Although larger than in other 9-MeA complexes such as $[(NH_3)_3Pt(9\text{-MeA-}N7)]^{2+}$ or *cis*-$[(NH_3)_2Pt(1\text{-MeC-}N3)(9\text{-MeA-}N7)]^{2+}$ (1-MeC = 1-methylcytosine),[29] this interaction shift is clearly smaller than that of free 9-MeA[29] or adenine nucleobases in general.[30] The reduction probably is a consequence of reduced stacking due to charge repulsion (+2 cations) and decreased nucleobase overlap due to the presence of a Pt moiety at the N7 site.

(27) Kistenmacher, T. J.; Orbell, J. D.; Marzilli, L. G. In *Platinum, Gold and Other Metal Chemotherapeutic Agents*; Lippard, S. J., Ed.; ACS Symposium Series 209; American Chemical Society: Washington, DC, 1983; pp 191−207.

(28) C.f. Figure 20 in: Lippert, B. *Prog. Inorg. Chem.* **1989**, *37*, 1.

(29) Beyerle-Pfnür, R. Ph.D. Thesis, Technical University Munich, 1985.

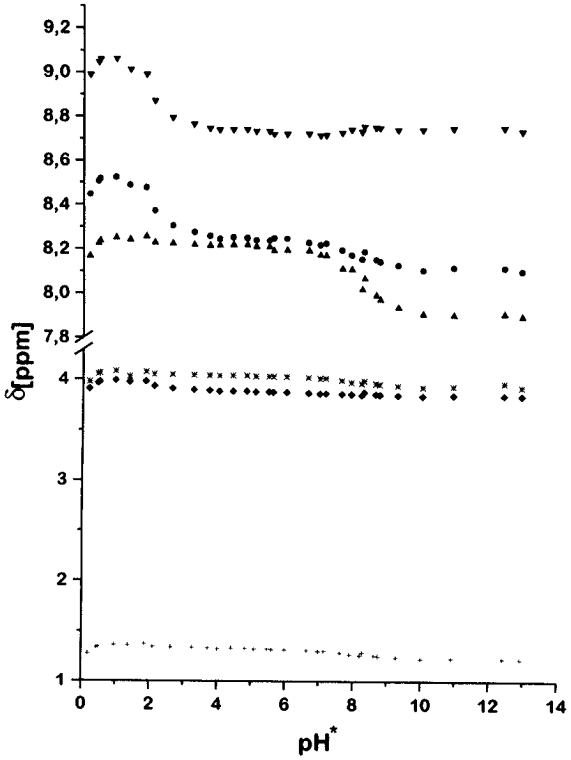

Figure 4. pH* dependence of ^{1}H NMR resonances of the title compound in D_2O: (▽) 9-MeA, H8; (○) 9-MeA, H2; (△) 9-EtGH, H8; (∗) 9-EtGH, $-CH_2-$; (◇) 9-MeA, $-CH_3$; (+) 9-EtGH, $-CH_3$.

The pH* dependence of the CH protons ($c_{Pt} \approx 0.04$ M) is given in Figure 4. It permits an unambiguous differentiation of adenine and guanine resonances. pK_a values for N1 protonated 9-MeA and for deprotonation of 9-EtGH at N1 are *ca.* 2.0 and 8.5, respectively. Below pH* 2 all guanine resonances undergo slight upfield shifts. This effect is probably due to a shift of the conformational equilibrium accompanying the N1 protonation of 9-MeA. That the protonation state of the nucleobases can modify the conformational preferences of a platinum bis(nucleobase) complex has been demonstrated in the case of *cis*-$[(NH_3)_2Pt\{r(GpG)\}]^+$.[9,14a]

In DMF-d_7, NH protons are also observed. Chemical shifts are as follows (ambient temperature, $c_{Pt} \approx 0.03$ M): 9-MeA, H8, 9.08 ppm; H2, 8.64 ppm; NH_2(6), 8.24 ppm; CH_3 3.92 ppm; 9-EtGH, N(1)H, 11.62 ppm; H8, 8.30 ppm; CH_2, 4.06 ppm; CH_3, 1.34 ppm. Spectra were recorded in this solvent between 233 and 349 K. Throughout this temperature range there are no indications of resonance doubling that could be interpretated in terms of hindered rotation about the Pt−*N7*(purine) bonds. Only at 233 K, the A−NH_2 resonance is split, consistent with a freezing-out of the rotation of the amino group. The observed slight downfield shifts of G−N(1)H, G−NH_2, and A−NH_2 with decreasing temperature are a consequence of H bonding interactions.

Conformational Analysis. The two main parameters defining the conformation of the complex *cis*-$[(NH_3)_2Pt(Ade)(Gua)]^{2+}$ are the torsion angles along the Pt−N7 bonds, α and *β* (Figure 1). Starting from the (hypothetical) square-planar structure shown in Figure 1, with nucleobase geometries taken from the AMBER database[23] and Pt−N bond lengths as determined for *cis*-$[(NH_3)_2Pt(9\text{-MeA})(9\text{-EtGH})]^{2+}$ (see above), i.e. Pt−NH_3, 2.03 Å; Pt−N7(Ade), 2.036 Å; Pt−N7(Gua), 2.006 Å, we have rotated the two bases about the Pt−N7 bonds by multiples of 10°. The nonbonded energy calculated with the AMBER forcefield (eq 1) yielded an energy map (Figure 5) similar to that obtained for the bis(guanine) complex.[9] However, because of the nonequivalence of the two bases, the map becomes less symmetrical. The remaining symmetry element is the center of symmetry relating enantiomeric pairs [α;*β*] and [−α;−*β*].

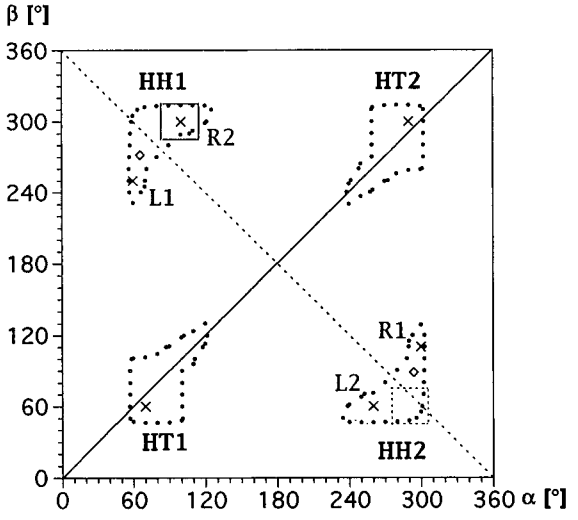

Figure 5. Calculated energy map for the *cis*-$[(NH_3)_2Pt(9\text{-MeA})(9\text{-EtGH})]^{2+}$ complex. × = energy minima; ◇ = [α;*β*] coordinates corresponding to the crystal structure of *cis*-$[(NH_3)_2Pt(9\text{-MeA})(9\text{-EtGH})]^{2+}$. Dots = level curves 4.8 kcal/mol (20 kJ/mol) above the R2 and L2 energy minima. Full-line square = proposed preferential domain of the major rotamer of *cis*-$[(NH_3)_2Pt\{d(ApG)\}]^+$. Dashed-line square = proposed preferential domain of the minor rotamer of *cis*-$[(NH_3)_2Pt\{d(ApG)\}]^+$. See Figure 1 for the definition of α and *β*.

In each of the *head-to-tail* (HT) zones (comprising structures with the two imidazole rings of the bases pointing to opposite sides of the coordination plane), there is only one energy minimum, lying 0.6 kcal/mol above the global minima. In addition, there are two shoulders located at [α;*β*] = [100°;100°] and [−100°;−100°] and lying 1.0 kcal/mol above the global minima.

In each of the *head-to-head* (HH) conformational zones (comprising structures with the two imidazole rings of the bases pointing to the same side of the coordination plane), there are two energy minima, labeled R2 and L1, and L2 and R1 (R indicates that the orientation of the bases is right-handed helicoidal and L means left-handed helicoidal). In the case of the bis(guanine) complex, *cis*-$[(NH_3)_2Pt(Gua)_2]^{2+}$, the four minima are equienergetic.[9] They correspond to conformations with one guanine inclined by ∼60° with respect to the coordination plane and forming a hydrogen bond between O6 and the NH_3 ligand in the *cis* position, and the other guanine close to perpendicular to the coordination plane (see Figure 3 of ref 9). It is clear that replacing the hydrogen-bonded guanine by adenine yields a structure which is not energetically equivalent to that resulting from replacement of the perpendicular guanine. Thus, in the energy map for *cis*-$[(NH_3)_2Pt(Ade)(Gua)]^{2+}$ (Figure 5), the two energy minima R2 and L2, corresponding to the replacement of the perpendicular guanine, are ∼1 kcal/mol lower in energy than the minima R1 and L1, corresponding to the replacement of the hydrogen-bonded guanine.

There is another difference distinguishing the HH1 and HH2 domains in the energy map of *cis*-$[(NH_3)_2Pt(Gua)_2]^{2+}$ from those calculated for *cis*-$[(NH_3)_2Pt(Ade)(Gua)]^{2+}$. In the former (Figure 2 of ref 9), the two minima (e.g. R2 and L1 in HH1) are separated by a saddle-point at midway between them (i.e.,

(30) See, e.g.: (a) Sigel, H. *Chimia* ***1987***, *41*, 11 and references cited therein. (b) Mitchell, P. R.; Sigel, H. *Eur. J. Biochem.* **1978**, *88*, 149. Dimicoli, J.-L.; Hélène, C. *J. Am. Chem. Soc.* **1973**, *95*, 1036. (d) Neurohr, K. J.; Mantsch, H. H. *Can. J. Chem.* **1979**, *57*, 1986.

Table 3. Calculated Chemical Shifts Due to Ring-Current Effects in *cis*-$[(NH_3)_2Pt(Ade)(Gua)]^{2+}$ [a]

beta [deg] \ alpha [deg]	40	50	60	70	80	90	100	110	120	130
	-0.01	-0.01	-0.02	-0.02	-0.03	-0.04	-0.06	-0.07	-0.09	-0.12
270	-0.25	-0.13	-0.06	-0.01	0.01	0.03	0.03	0.04	0.04	0.04
	0.20	0.19	0.17	0.14	0.10	0.06	0.01	-0.03	-0.06	-0.08
	-0.01	-0.02	-0.02	-0.03	-0.04	-0.05	-0.07	-0.08	-0.10	-0.12
280	-0.12	-0.02	0.03	0.05	0.06	0.06	0.06	0.06	0.05	0.05
	0.23	0.22	0.20	0.15	0.10	0.04	-0.01	-0.06	-0.11	-0.13
	-0.01	-0.02	-0.03	-0.03	-0.04	-0.06	-0.07	-0.09	-0.10	-0.12
290	0.03	0.09	0.11	0.11	0.10	0.10	0.09	0.08	0.07	0.06
	0.27	0.26	0.22	0.16	0.09	0.02	-0.06	-0.12	-0.17	-0.21
	-0.01	-0.02	-0.03	-0.03	-0.04	-0.06	-0.07	-0.08	-0.10	-0.11
300	0.17	0.18	0.17	0.16	0.14	0.12	0.11	0.09	0.08	0.07
	0.32	0.30	0.24	0.17	0.07	-0.03	-0.12	-0.21	-0.27	-0.31
	-0.01	-0.01	-0.02	-0.03	-0.04	-0.05	-0.06	-0.07	-0.08	-0.09
310	0.27	0.25	0.22	0.19	0.16	0.14	0.12	0.10	0.09	0.08
	0.38	0.34	0.26	0.15	0.02	-0.11	-0.23	-0.32	-0.40	-0.44
	0.00	-0.01	-0.02	-0.02	-0.03	-0.04	-0.05	-0.06	-0.07	-0.07
320	0.34	0.29	0.24	0.20	0.17	0.14	0.12	0.11	0.10	0.09
	0.44	0.36	0.24	0.09	-0.08	-0.24	-0.38	-0.49	-0.57	-0.61
	0.00	0.00	-0.01	-0.01	-0.02	-0.03	-0.03	-0.04	-0.04	-0.04
330	0.36	0.30	0.24	0.20	0.16	0.14	0.12	0.11	0.10	0.09
	0.48	0.35	0.18	-0.03	-0.24	-0.42	-0.57	-0.69	-0.76	-0.79
beta [deg] \ alpha [deg]	40	50	60	70	80	90	100	110	120	130

[a] Key: upper line, (de)shielding of H2(Ade) due to guanine; middle line, (de)shielding of H(8)(Ade) due to guanine; lower line, (de)shielding of H8(Gua) due to adenine. Shifts are given for α between 40 and 130° and β between 270 and 330°. For the other values of α and β see Table A2 in the Supporting Information. See Figure 1 for the definition of α and β. Downfield shifts are positive.

at $[\alpha;\beta] = [75°;-75°]$ in HH1), laying 1.2 kcal/mol above the two minima. In the latter (Figure 5), the separating saddle-point is located very close to the upper minimum L1 or R1 (i.e., at $[\alpha;\beta] = [65°;-95°]$ in HH1), and lies only 0.2 kcal/mol above it. In other words, whereas in the energy landscape of *cis*-$[(NH_3)_2Pt(Gua)_2]^{2+}$, the diagonal separating the right- and left-handed structures (analogous to the dashed diagonal in Figure 5) corresponds to a ridge, in the energy landscape of *cis*-$[(NH_3)_2Pt(Ade)(Gua)]^{2+}$, the well around R2 (and L2) is very flat and extends beyond the diagonal, so that passing from right-handed helicity to left-handed does not coincide with passing an energy barrier. The difference is due to the fact that the O6(G)−O(6)G repulsion which causes the ridge in the bis-(guanine) complex is replaced by an NH_2(A)−O6(G) attraction in the case of the adenine-guanine complex. In line with this, in the crystal structure of *cis*-$[NH_3)_2Pt(9\text{-MeA})(9\text{-EtGH})]^{2+}$, for which the $[\alpha;\beta]$ values lie close to the dashed diagonal (Figure 5), NH_2(A)−O6(G) hydrogen bonding is observed (*vide supra*).

Calculation of H2 and H8 Chemical Shifts. Application to the Solution Structure of the Two Rotamers of *cis*-$[(NH_3)_2Pt\{d(ApG)\}]^+$. The ring current effect of one base on the aromatic protons of the other base was calculated using the method developed by Giessner-Prettre and Pullman.[31] Table A2 of the Supporting Information gives the ring current shifts as a function of the two angles α and β, and Table 3 provides the section most relevant to the following discussion.

If the *cis*-$[(NH_3)_2Pt(9\text{-MeA})(9\text{-EtGH})]^{2+}$ complex had a fixed geometry in solution, the measurement of the H2 and H8 chemical shifts would allow the determination of the torsion angles α and β. In reality, however, the bases in platinum−bis(nucleobase) complexes undergo rotations about the Pt−N7 bond which, at least in the case of guanines, are fast on the NMR time scale.[12] Thus, the observed chemical shifts reflect a complicated equilibrium between structures belonging to the four low-energy domains (Figure 5). On the other hand, when the adenine and the guanine bound to platinum are, in addition, linked together by a sugar-phosphate backbone, such as in the dinucleotide complexes *cis*-$[(NH_3)_2Pt\{r(ApG)\}]^+$ or *cis*-$[(NH_3)_2Pt\{d(ApG)\}]^+$, the rotations about the Pt−N7 bonds are severely restricted and rotamers belonging to distinct low-energy domains can be observed. Such is the case of *cis*-$[(NH_3)_2Pt\{d(ApG)\}]^+$, for which two sets of signals appear in the the NMR spectrum, indicating two conformers interconverting slowly on the NMR time scale.[32] In the following, we show how the calculated ring current effects can be used to assign the two sets of NMR peaks to two of the four low-energy domains.

The chemical shifts of the aromatic protons, measured for *cis*-$[(NH_3)_2Pt\{d(ApG)\}]^+$ at pH* = 4.5, are as follows.[32] Major rotamer: H8(A), 9.23; H2(A), 8.25; H8(G) 8.45 ppm. Minor rotamer: H8(A), 9.30; H2(A), 8.30; H8(G) 8.80 ppm. If we assume that the chemical shifts are determined mainly by the inductive effect of platinum and the ring current effect of the other base, we can approximate the δ values as in eq 2.

$$\delta(H_i, \textit{cis}\text{-}[(NH_3)_2Pt\{d(ApG)\}]^+) = \delta(H_i, \text{free nucleoside}) + \Delta_{ind} + \Delta_{rc} \quad (2)$$

From the known shifts in the free nucleoside and the inductive effect Δ_{ind}, the ring current effect Δ_{rc} on each proton can be calculated. Taking as reference the values for deoxyguanosine and deoxyadenosine, i.e. H8(A), 8.32; H2(A), 8.23; and H8-(G), 8.00 ppm,[33] with the inductive effects due to coordination of *cis*-$[(NH_3)_2PtL_2]^{2+}$ (L = neutral ligand) determined previously,[33] i.e. H8(A), +0.68; H2(A), +0.09; and H8(G), +0.52 ppm, we obtain the following results for the ring current effects Δ_{rc}. Major rotamer: H8(A), +0.23; H2(A), −0.07; H8(G) −0.07 ppm. Minor rotamer: H8(A), +0.30; H2(A), −0.02; H8(G), +0.28 ppm.

These ring current effects can now be compared with those calculated for the different conformations of the core complex *cis*-$[(NH_3)_2Pt(Ade)(Gua)]^{2+}$ in order to see to which low-energy domains the Δ_{rc} values correspond. For this purpose, Table A2 (and Table 3, respectively) has to be consulted together with Figure 5, bearing in mind that Table A2 (Table 3) represents only one half-space, and that to each conformation $[\alpha,\beta]$ a corresponding $[-\alpha,-\beta]$ conformation exists, for which the ring current effects are the same. We observe that the deshielding of H8(A) and shielding of H8(G) and H2(A) is consistent with the conformational domain centered around the energy minimum R2 in the zone HH1 (marked with a full-line square in Table A2 and Table 3). The corresponding domain in the HH2 zone, centered around the energy minimum L2, gives, of course, the same accord. The minor rotamer differs from the major rotamer mainly in the resonance of H8(G) which is apparently deshielded by the adenine. Inspection of Table A2 (Table 3) shows that a conformational domain with both H8 protons deshielded, and H2(A) slightly shielded exists in the HH1 zone, close to R2 (marked with a dashed-line square in Table A2). This domain, again, has a counterpart in the HH2 zone, close to the energy minimum L2. It is, of course, not possible to assign the full-line-square domain and the dashed-line-square domain of the same zone (say HH1) to the two rotamers, since in such a case, they would interconvert rapidly and could not be observed separately. However, it is conceivable that the major rotamer corresponds to the full-line square of one HH zone and the minor rotamer to the dashed-line square of the other HH zone. Both

(31) Giessner-Prettre, C.; Pullman, B. *Q. Rev. Biophysics* **1987**, *20*, 113.
(32) Dijt, F. J.; Chottard, J. C.; Girault, J. P.; Reedijk, J. *Eur. J. Biochem.* **1989**, *179*, 344.
(33) Lemaire, D.; Fouchet, M. H.; Kozelka, J. *J. Inorg. Biochem.* **1994**, *53*, 261.

HH zones are separated by a substantial energy barrier which slows down the interconversions. Which rotamer belongs to which HH zone is impossible to conclude from the analysis of the chemical shifts alone. However, an assignment is feasible based on the fact that the base orientations corresponding to the minima R2 and L2 have opposed helicities. The CD spectrum of the ribodinucleotide analogue, *cis*-[$(NH_3)_2$Pt{r(ApG)}]$^+$, which is conformationally pure and whose NMR signals are very close to those of the major rotamer of *cis*-[$(NH_3)_2$Pt{d(ApG)}]$^+$, indicates a right-handed helicity.[18a] Thus, we attribute the major rotamer to the conformational full-line-square domain around the R2 minimum (HH1), and the minor rotamer to the dashed-line-square domain close to L2 (HH2). The two squares, representing the conformational domains of the two rotamers, have been transposed into Figure 5, in order to show how they fit into the HH zones.

The fact that the conformational domain of the minor rotamer does not correspond exactly to the mirror image of that of the major rotamer (that means, the full-line and dashed-line squares in Figure 5 are not related by the center of symmetry) is not surprising, since the bottoms of the energy wells around the R2 and L2 minima in the energy map of the core *cis*-[$(NH_3)_2$Pt(Ade)(Gua)]$^{2+}$ complex are very flat. The constraints of the sugar−phosphate backbone, which can be fairly different in the HH1 and HH2 rotamers, probably account for the deviations from an exactly enantiomeric relationship between the base orientations in the two rotamers.

The orientation of the nucleobase in the two enantiomeric forms of the reported crystal structure are [$\alpha;\beta$] = [66°;−88°] and [$\alpha;\beta$] = [−66°;88°]. The two conformations belong to the two domains HH1 and HH2, respectively (Figure 5). Although the [$\alpha;\beta$] values are closer to those of the L1 and R1 minima than those of R2 and L2, in the energy landscape, these conformations still belong to the wells containing R2 and L2 minima, which, as stated above, are extended beyond the dashed diagonal. As obvious from Figure 5, the [$\alpha;\beta$] values of the HH2 enantiomer of *cis*-[$(NH_3)_2$Pt(9-MeA)(9-EtGH)]$^{2+}$ are closer to the dashed-line square domain than are the [$\alpha;\beta$] values of the HH1 enantiomer to the full-line square. Therefore, the HH2 form of of *cis*-[$(NH_3)_2$Pt(9-MeA)(9-EtGH)]$^{2+}$ is a better model for the minor rotamer of *cis*-[$(NH_3)_2$Pt{d(ApG)}]$^+$ than is the HH1 form for the major rotamer.

Relevance of this Study to the Modeling of Cisplatin−DNA Adducts

Platinum−DNA adducts can be modeled at different levels. Bis(nucleobase) complexes, the simplest models, yield information about the coordination sphere of the metal. On the other end of the scale, platinum−oligonucleotide complexes are the most sophisticated models, in which the DNA part is simply shortened and lacks tertiary structure.

Platinum−dinucleotide complexes are intermediate models which contain a sugar−phosphate backbone but are sufficiently small to be studied in detail by spectroscopic and in favorable cases by crystallographic techniques. Their structural data can be compared, on the one hand, with those of bis(nucleobase)-complexes and on the other hand, with those of platinum−oligonucleotide complexes. Such a comparison between the three available crystal structures of *cis*-[$(NH_3)_2$Pt(9-EtGH)$_2$]$^{2+}$,[11] NMR and (in the latter case) X-ray data for the dinucleotide complexes *cis*-[$(NH_3)_2$Pt{d(GpG)}]$^+$,[14] *cis*-[$(NH_3)_2$Pt{r(GpG)}]$^+$,[14a] and *cis*-[$(NH_3)_2$Pt {d(pGpG)},[14a,15] and NMR data for oligonucleotide d(GpG) adducts of *cis*-$(NH_3)_2Pt^{2+}$ (reviewed in ref 9) have allowed to conclude that the preferential orientations of the two nucleobases are mainly determined by the ligand−ligand forces within the coordination sphere and that the sugar−phosphate backbone of an oligonucleotide complex mainly determines *which* of these preferential orientations is (are) finally preponderant.[9]

Concerning modeling of the d(ApG)−platinum crosslink, the second major adduct found in cisplatin-modified DNA, extended spectroscopic work has been carried out on the dinucleotide complexes *cis*-[$(NH_3)_2$Pt{d(ApG)}]$^+$ [28] and *cis*-[$(NH_3)_2$Pt{r(ApG)}]$^+$,[18a] but it was not possible so far to translate the NMR data into three dimensional structures. Specifically, it has been shown that *cis*-[$(NH_3)_2$Pt{d(ApG)}]$^+$ exists in solution as an equilibrium of two rotamers, but the orientation of the two nucleobases with respect to the platinum coordination plane could not be determined. Also, no crystal structures of mixed adenine,guanine platinum complexes have been reported to date. In this work, we have partly filled up this gap and present (i) the first crystal structure analysis of a complex containing 9-methyladenine and 9-ethylguanine bound to platinum and (ii) a conformational analysis allowing the attribution of the major and minor rotamers of *cis*-[$(NH_3)_2$Pt{d(ApG)}]$^+$ to the head-to-head domains HH1 and HH2, respectively. The two enantiomeric conformations found in the crystal structure of of *cis*-[$(NH_3)_2$Pt(9-MeA)(9-EtGH)]$^{2+}$ correspond to the HH1 and HH2 zones, respectively. The orientation of the bases is such that the HH2 form is close to what we believe, based on chemical shifts calculations, to be the conformational domain of the minor rotamer of *cis*-[$(NH_3)_2$Pt{d(ApG)}]$^+$ (dashed-line square in Figure 5). On the other hand, the HH1 crystal form is a less good model for the major rotamer of *cis*-[$(NH_3)_2$Pt{d(ApG)}]$^+$, which the chemical shifts considerations indicate to have base orientation corresponding to a domain centered around the R2 energy minimun (full-line square in Figure 5).

In double-stranded adducts with *cis*-$(NH_3)_2Pt^{2+}$, the double helix is likely to favor the right-handed conformation "R2" of the domain HH1. Thus, the crystal structure of *cis*-[$(NH_3)_2$Pt-(9-MeA)(9-EtGH)]$^{2+}$ reported here probably does not represent a model for d(ApG)−platinum crosslinks occuring in duplex DNA. Attempts to crystallize the *cis*-[$(NH_3)_2$Pt(9-MeA)(9-EtGH)]$^{2+}$ complex with other counterions and/or in different conditions, with the hope to obtain an "R2" structure, are underway.

Acknowledgment. This work was supported by the Deutsche Forschungsgemeinschaft, the Fonds der Chemischen Industrie, and Asta Medica. M.-H.F. and J.K. were supported by the Association pour la Recherche sur le Cancer.

Supporting Information Available: Tables of crystallographic data, positional parameters, thermal displacement parameters, intermolecular distances, torsional angles, least-square planes, atomic charges used in the molecular mechanics calculations (Table A1), and calculated chemical shifts (Table A2) and a figure showing the concentration dependency of chemical shifts (15 pages). Ordering information is given on any current masthead page.

IC950754S